ELSEVIER

Kinetics of mercury ions removal from synthetic aqueous solutions using by novel magnetic p(GMA-MMA-EGDMA) beads

Gülay Bayramoğlu*, M. Yakup Arica

Biochemical Processing and Biomaterial Research Laboratory, Faculty of Science, Kırıkkale University, 71450 Yahşihan, Kırıkkale, Turkey

Abstract

Poly(glycidylmethacrylate-methylmethacrylate), p(GMA-MMA-EGDMA), magnetic beads were prepared via suspension polymerization in the presence of ferric ions. The epoxy groups of the beads were converted into amino groups via ring opening reaction of the ammonia and, the aminated magnetic beads were used for the removal of Hg(II) ions from aqueous solution in a batch experiment and in a magnetically stabilized fluidized bed reactor (MFB). The magnetic p(GMA-MMA-EGDMA) beads were characterized with scanning electron microscope (SEM), FT-IR and ESR spectrophotometers. The optimum removal of Hg(II) ions was observed at pH 5.5. The maximum adsorption capacity of Hg(II) ions by using the magnetic beads was 124.8 ± 2.1 mg g^{-1} beads. In the continuous MFB reactor, Hg(II) ions adsorption capacity of the magnetic beads decreased with an increase in the flow-rate. The maximum adsorption capacity of the magnetic beads in the MFB reactor was 139.4 ± 1.4 mg g^{-1}. The results indicate that the magnetic beads are promising for use in MFB for removal of Hg(II) ions from aqueous solution and/or waste water treatment.
© 2006 Elsevier B.V. All rights reserved.

Keywords: Magnetic beads; Hg(II) ions; Removal; Adsorption; Kinetic

1. Introduction

Aqueous waste streams from ore mining processes are contaminated with high concentrations of toxic heavy metal ions. In the area of the removal of heavy metal ions from aqueous solution and/or contaminated water is usually performed using variety of conventional procedure, electrophoretic, ultrafiltration, reverse osmosis, ion exchange, chemical precipitation and other procedures, adsorption being one of the most important techniques [1,2]. The adsorption of mercury ions has been extensively investigated using various polymeric materials [3–5]. The acrylic polymers are almost ideal ones to perform, very stable in a range of buffers from pH 1 to 10 and were resistant to microbial degradation and several chemicals [5,6]. In addition, magnetic separation technique, using magnetic polymeric particles, is quick and easy method for sensitive and reliable capture of inorganic or organic pollutants. These methods are also non-laborious, cheap and often highly scalable. Moreover,

techniques employing magnetism are more amenable to automation and miniaturization [7]. The most well known technique is the magnetically stabilized fluidized bed reactor (MFB). MFB reactor uses an externally applied, axially or transversely aligned magnetic field to independently control the magnetic particles movement in a column [8,9]. Magnetically stabilized fluidized bed exhibits combination of the best characteristics of both packed and fluidized bed reactor design [9].

Mercury is a remarkably toxic and accumulates in the biosystem and can be regenerated by several sources, resulting in contamination of atmospheric and aqueous systems [2,3,10]. The toxic effects of mercury depend on its chemical form and the route of exposure. The main sources of mercury emissions to land, water and air are the processes of ores mining and smelting (in particular Cu and Zn smelting), burning of fossil fuels (mainly coal), industrial production processes (mercury cells and chlor-alkali processes for the production of Cl) and consumption related discharges (including waste incineration) [11]. Considerable attention for Hg(II) ions, which damages the gastrointestinal tract and causes kidney failure, is unlikely from environmental sources. The prescribed limit of 0.001 ppm for mercury is the lowest among all heavy metal ions [12].

* Corresponding author. Tel.: +90 318 357 2477; fax: +90 318 357 2329.
E-mail address: gbayramoglu@kku.edu.tr (G. Bayramoğlu).

In this study, magnetic beads were prepared from glycidyl-methacrylate (GMA) and methylmethacrylate (MMA) in the presence of a cross-linker (i.e., ethyleneglycol dimethacrylate, EGDMA) via suspension polymerization. The functional epoxy groups of the beads were converted into amino groups. The size and structure of the beads were characterized using SEM and FT-IR spectroscopy, respectively. In addition, surface area measurement, swelling test, and electron spin resonance (ESR) were used for further characterization of the magnetic beads. The aminated magnetic beads were used for the removal of Hg(II) ions from aqueous solution and the optimum adsorption conditions in a batch system were evaluated. The adsorption isotherm and kinetic models was measured in order to evaluate the discrepancy between the experimental data and the theoretical equilibrium capacity predicted from the model equations. Finally, the magnetic beads were applied to a magnetically stabilized fluidized bed reactor (MFB) under different flow-rate conditions for removal of Hg(II) ions.

2. Material and method

2.1. Materials

Methyl methacrylate (MMA), glycidyl methacrylate (methacrylic-acid 2,3-epoxypropyl-isopropyl-ether; (GMA), ethyleneglycol-dimethacrylate (EGDMA), α-α'-azoisobisbuty-ronitrile (AIBN), polyvinyl alcohol (PVA) and toluene were supplied from Sigma Chemical Co. (St. Louis, MO, USA). The monomers distilled under reduced pressure in the presence of hydroquinone and stored at 4 °C until use. All other chemicals were of analytical grade and were purchased from Merck AG (Darmstadt, Germany). The water used in the present work was purified using a Barnstead system (Dubuque, IA, USA).

2.2. Preparation of magnetic p(GMA-MMA-EGDMA) beads

The magnetic p(GMA-MMA-EGDMA) beads were prepared in two sequential steps. In the first step, ferric-p(GMA-MMA-EGDMA) beads were prepared via suspension polymerization, which was carried out in an aqueous dispersion medium containing FeCl$_3$ (0.3 M, 400 ml; it was used as a precursor for the thermal iron oxide precipitation in the beads). The organic phase contained GMA (7.5 ml), MMA (7.5 ml), EGDMA (7.5 ml; as cross-linker) and 5.0% polyvinyl alcohol (20 ml, as stabilizer) were mixed together with 0.2 g of AIBN as initiator in 20 ml of toluene. The polymerization reactor was placed in a water bath and heated to 65 °C. The reactor was then equipped with a mechanical stirrer, nitrogen inlet and reflux condenser. The polymerization reaction was maintained at 70 °C for 2.0 h and then at 80 °C for 1.0 h. After the reaction, the resultant beads were filtered under suction and washed with distilled water and ethanol. In the second step, magnetizations of the p(GMA-MMA-EGDMA) beads were performed by conventional co-precipitation reaction of iron oxide in the beads. For the co-precipitation reaction, 5.0 g FeCl$_2$ was dissolved in purified water (100 ml) and then was transferred into a reactor contain-

ing ferric-p(GMA-MMA-EGDMA) beads (15 g) in NH$_3$·H$_2$O (50 ml, 25% w/v). The reactor was equipped with reflux condenser and refluxed under nitrogen atmosphere at 40 and 50 °C for 2 h, and then at 90 °C for 2 h while continuous stirring. Finally, the synthesized magnetic p(GMA-MMA-EGDMA) beads were separated from the reaction medium, washed in ethanol solution (70%; 250 ml) for 3 h, and then washed with purified water. During the thermal co-precipitation reaction, the epoxy groups of the magnetic beads were also converted into amino groups via ring opening reaction due to the presence of ammonia in the medium. During washing, the magnetic beads were separated from the solutions using a magnetic separator. The beads were finally dried in a vacuum oven at 50 °C and stored at room temperature until use.

2.3. Characterization of magnetic beads

The amount of available surface functional epoxy groups content of the magnetic p(GMA-MMA-EGDMA) beads was determined by pyridine–HCl method as described previously [6]. The amount of amine group content of the magnetic beads was determined by potentiometric titration. The magnetic beads (0.2 g) was allowed soak into water (10 ml) for 24 h. Then, 2 M HCl (10 ml) was added to the mixture and shaken for 1 h. At the end of this period the beads filtered and assayed by titration with 2 M NaOH solution.

The average size and size distribution of the magnetic beads were determined by screen analysis performed by using molecular sieves. The specific surface area of the beads was measured by a surface area apparatus and calculated using the BET (Brunauer, Emmett and Teller) method. Scanning electron micrographs (SEM) of the dried magnetic beads were obtained using a JEOL, JMS 5600 scanning electron microscope, after coating with gold under reduced pressure. The FT-IR spectra of the magnetic beads were obtained using an FT-IR spectrophotometer (Shimadzu, FT-IR 8000 Series, Japan). Electron spin resonance (ESR) spectroscopy was carried out with a conventional X-band ($\nu = 9.75$ Hz) Bruker ESP 300E spectrometer at 100 kHz magnetic field modulation frequency, 31.7 G modulation amplitude and 0.1 mW microwave power. The magnetic p(GMA-MMA-EGDMA) beads about (50 mg) were placed into quartz tube and the measurements were performed at room temperature. The first derivative of the power absorption had been recorded as a function of the applied magnetic field.

2.4. Adsorption studies

The effects of adsorption equilibrium time, the pH of the medium and initial concentration of Hg(II) ions on the adsorption capacity of the aminated magnetic beads were studied in batch experimental mode. Nitrate of the mercury ions was used throughout the adsorption experiments. Aqueous solutions (50 ml) containing different amounts of Hg(II) ions (20–600 mg L^{-1}) were incubated with magnetic beads at different pH (in the pH range of 2.0–6.0, which was adjusted with HNO$_3$ or NaOH at the beginning of experiments and not

controlled afterwards) at 25 °C (performed in a temperature-control chamber), in flasks agitated magnetically at an agitation speed of 600 rpm. Blank trials without magnetic beads addition were performed for each tested Hg(II) ions concentrations. After the desired adsorption periods (up to 120 min), the magnetic beads were separated from aqueous phases and the residual concentrations of the metal ions in the aqueous phases were measured by atomic absorption spectrophotometer and employed a cold mercury vapor unit. Deuterium background correction was applied throughout the experiments and the spectral slit width was 0.7 nm. The working current/wavelength values and the optimized experimental conditions for mercury measurements were as follows: working current/wavelength, 6 mA/253.6 nm; concentration of $SnCl_2$, 1% (w/v); concentration of $KMnO_4$, 0.5% (w/v); concentration of H_2SO_4, 5% (w/v). The instrument response was periodically checked with known heavy metal solution standards. For each sample, the mean of 10 measurements was recorded. For each set of data present, standard statistical methods were used to determine the mean values and standard deviations. Confidence intervals of 95% were calculated for each set of samples in order to determine the margin of error. The amount of Hg(II) ions adsorbed per unit mass of material (mg metal ions/g beads) was calculated by using the determination data in described earlier [6].

2.5. Magnetically stabilized fluidized bed reactor operation

Adsorption of Hg(II) ions onto magnetic beads were also performed in a magnetically stabilized fluidized bed reactor. The magnetic beads were equilibrated in the purified water at pH 5.5 for 6 h and they were degassed under reduced pressure (by using water suction pump). The magnetically stabilized reactor with a water jacket was constructed from Pyrex glass (height 80 mm; inner diameter: 12 mm, total volume; about 9.0 ml). It was equipped with Helmholtz coils (Model HC-1.5, Magnetic Instrumentation, Indianapolis, USA) and equilibrated beads about 6 g was transferred into MFB reactor. The void volume of the reactor was about 3.0 ml. The Hg(II) ions solution (200 mg L^{-1}) was pumped through the lower inlet part of the reactor by using a peristaltic pump at different flow-rate between 20 and 120 ml h^{-1}. The effluent leaving from the reactor was collected by means a fraction collector and the concentrations of the Hg(II) ions in these solutions were measured as described above.

The dynamic adsorption capacity of the magnetic beads for Hg(II) ions in the column was calculated by mass balance:

$$q = \frac{[(C_o - C)V\rho_w]}{W} \tag{1}$$

where, C_o and C (mg L^{-1}) are the initial and final Hg(II) ions concentration in the feed and effluent, respectively; V (L) is the total volume of the feed and collected effluent; W (g) and ρ_w (g L^{-1}) stand for the weight and density of the wet magnetic beads, respectively. Here, ρ_w was determined with a pycnometry in n-decane.

3. Results and discussion

3.1. Characterization of magnetic beads

The preparation of magnetic beads were carried out under two sequential steps: in the first, the ferric ions containing p(GMA-MMA-EGDMA) beads were prepared from GMA and MMA monomers via suspension polymerization in the presence of the ferric ions. In the second step, the classical thermal co-precipitation reaction was carried out in $NH_3 \cdot H_2O$ aqueous solution containing Fe^{2+} ions for the formation of iron oxide crystal within the structure of the beads. The beads were sieved and 75–150 μm size of fraction was used in the further reactions. The specific surface area of the magnetic p(GMA-MMA-EGDMA) beads was measured by BET method and was found to be 21.6 m^2 g beads^{-1}. The amount of available epoxy groups on the p(GMA-MMA-EGDMA) beads surface was determined by HCl–pyridine method and was found to be 1.12 mmol g beads^{-1}. GMA monomer was use initially to incorporate epoxy groups on the polymer surface for further modification of the beads. The obtained value for epoxy groups was lower than that of the theoretical value (2.59 mmol g^{-1}) because some of the epoxy groups remain inside of the magnetic beads and are not accessible for subsequent reactions or analytical determinations. The water content is very important when use of the support material in continuous column application is contemplated. The equilibrium-swelling ratio of the magnetic p(GMA-MMA-EGDMA) beads was determined as 1.39 weight basis. The magnetic p(GMA-MMA-EGDMA) beads density was measured to be 1.32 g cm^{-3}.

The magnetic properties of the beads were confirmed with electron spin resonance spectroscopy (ESR) at room temperature and the intensity versus the magnetic field (G) (Fig. 1). The spectrum has two component: (i) a typical low field high intensity ferromagnetic resonance signal (below 2000 G), and (ii) a broad line pick extended up to 5000 G. In this ESR spec-
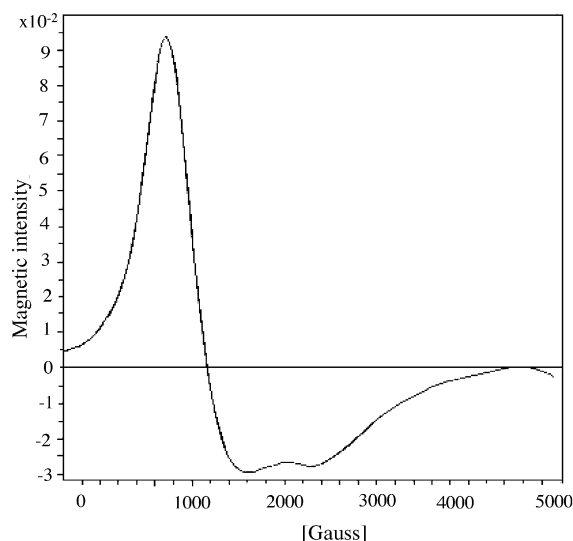

Fig. 1. Electron spin resonance (ESR) spectrum of magnetic p(GMA-MMA-EGDMA) beads at room temperature.
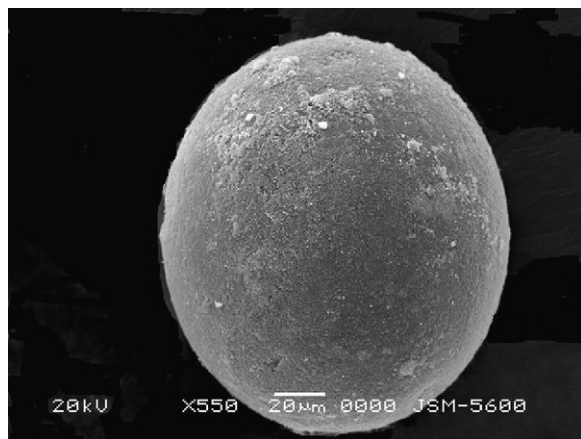
Fig. 2. SEM micrograph of the magnetic p(GMA-MMA-EGDMA) beads.

trum, about 1000 G magnetic field was found to be sufficient to excite all of the dipole moments of the sample beads that consist of magnetite. The value of this magnetic field is a function of the flow velocity, particle size and magnetic susceptibility of the beads to be displaced. In the literature, the value was reported up to 20,000 G [13], so the magnetic beads developed in this study will need less magnetic intensity for various reactor configurations. So, the magnetic beads can be easily separated within a few second by a conventional permanent magnet. When the applied magnetic force is removed, the magnetic beads can easily be dispersed by simple shaking. Thus, the magnetic beads can be removed or recycled in the separation medium. The presented spectrum was similar to ESR spectra of iron (III) nanoparticles in alginate polymer [14]. Scanning electron microscopy (SEM) micrographs presented in Fig. 2 shows the porous surfaces structure of the magnetic p(GMA-MMA-EGDMA) beads. The beads have a spherical form and rough surface due to the pores, which formed during the polymerization process. The metal ions should be adsorbed both the external surface of the beads and within the pore space near the surface, and thus provided a large surface area for the removal of Hg(II) metal ions. The FT-IR spectra of the aminated magnetic beads have the characteristic stretching vibration band of hydrogen-bounded alcohol at ∼3500 cm^{-1} (Fig. 3). Among the characteristic vibrations of both GMA and MMA is the methylene vibration at ∼2953 cm^{-1}. The vibration at 1731 cm^{-1} represents the car-

bonyl band of both MMA and GMA. The epoxide group gives the band between at 910 cm^{-1} (epoxy ring vibrations). The FT-IR spectra of the aminated magnetic beads have characteristic N–H amine stretching bands at 3500 and 1655 cm^{-1} are is due to amino groups bonded to the magnetic beads. Fe_3O_4 has the characteristic band at 600 cm^{-1} and also this indicates that Fe_3O_4 molecules are successfully introduced within the structure of p(GMA-MMA-EGDMA) beads. This was also confirmed by gravimetric analysis and the amount of precipitated iron oxide crystal in the bead structure was 134 mg g^{-1} beads. The magnetic beads were also incubated in the pH ranges 2–10 for 48 h using 0.1N HCl and 0.1N NaOH for adjusting pH. After this period, the magnetic beads were dried and Fe content was determined by gravimetrically. It was observed no significant change in Fe content in the pH range 2–10.

3.2. Effect of pH

Several studies showed that metal ion adsorption onto nonspecific and specific adsorbents are pH dependent [15–17]. In the absence of complexing agents, the hydrolysis and precipitation of the metal ions are affected by the concentration and form of soluble species. The solubility of metal ions is governed by hydroxide or carbonate concentration. According to the hard and soft acid–base theory, Hg(II) is classified as a soft metal ions and selectively interact with nitrogen and sulfur atoms of the molecules (such as R–CN, R–SH, R–NH$_2$ and imidazole groups) [4,18]. The performance of the adsorbent was studied in the pH range of 2.0–6.0 at 25 °C (Fig. 4). As seen in this figure, by adsorption of Hg(II) ions by the adsorbent was increased with increasing pH from 2.0 to 5.0 and then reached a plateau value of about pH 5.5. Lower adsorption capacity at lower pH values can be attributed to the competitive adsorption between H$_3$O$^+$ and Hg(II) ions for the same interactive adsorption sites. The functional amino groups of the magnetic beads should have taken part in metal removal process by complexation which is pH dependent, and both the nature of the binding sites of adsorbent
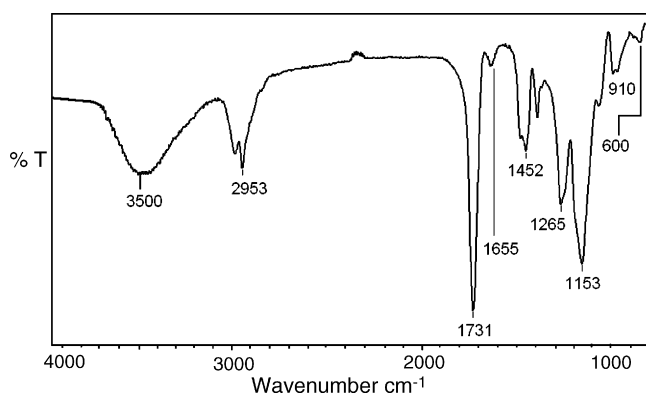

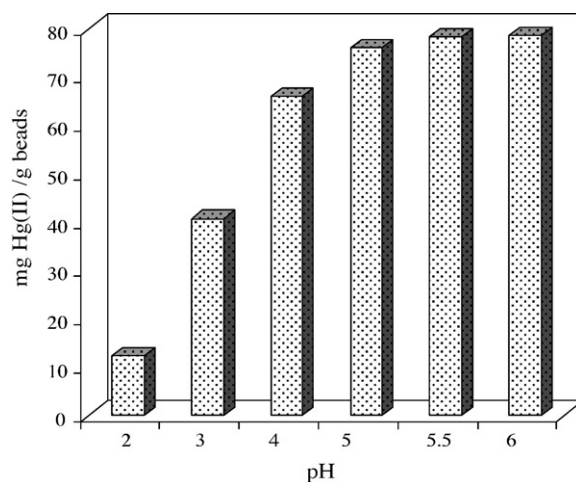Fig. 3. FT-IR spectrum of the magnetic p(GMA-MMA-EGDMA) beads.

Fig. 4. Effect of pH on the Hg(II) adsorption onto magnetic beads; initial concentration of metal ions: 100 mg L^{-1}; volume of the medium: 50 mL; temperature: 298 K.

and the chemistry of the metal ions should have been changed with pH of the medium. The adsorption capacity of the adsorbent to Hg(II) ions reached a maximum at pH 5.5. In the remaining experiment, this optimum pH value was used.

3.3. Equilibrium isotherm models

To obtain the maximum adsorption capacity for the aminated magnetic beads, the initial concentrations of Hg(II) ion was increased up to 400 mg L^{-1} (Fig. 5). The amount of Hg(II) ions adsorbed per unit mass of the beads increased with the increase in the initial concentration of metal ions, as expected. This behavior can be explained with the high driving force for the mass transfer. Thus, the maximum adsorption capacity of the beads was found to be 124.8 ± 2.1 mg g^{-1}.

Equilibrium data, commonly known as adsorption isotherms, are the basic requirements for the design of adsorption systems [19–21]. Obtaining equilibrium data for a specific adsorbate/adsorbent system can be performed experimentally, with a time-consuming procedure that is incompatible with the growing need for adsorption systems design. Analysis of equilibrium data is important for characterize the interaction of Hg(II) ions with the amino groups of the magnetic beads. This provides a relationship between the concentration of metal ions in the adsorption medium and the amount of metal ions adsorbed on the solid-phase when the two phases are at equilibrium. Among the several isotherm equations, two isotherms (Langmuir and Freundlich adsorption isotherms) were investigated, which are widely used to analyses data for water and wastewater treatment applications. The Langmuir equation is:

$$q_e = \frac{q_m b C_e}{1 + b C_e} \tag{2}$$

where C_e and q_e also show the residual metal concentration (mg L^{-1}) and the amount of metal adsorbed on the adsorbent at equilibrium (mg g^{-1}), respectively, b is the energy of adsorption

or adsorption equilibrium constant (L mg^{-1}) of the system. The maximum adsorption capacity, q_m, is the solid-phase concentration corresponding to a condition in which all available sites are filled. The essential features of a Langmuir isotherm can be expressed in terms of a dimensionless constant separation factor or equilibrium parameter, R_L, which is used to predict if an adsorption system is "favorable" or "unfavorable" [22,23].

$$R_L = \frac{1}{1 + b C_o} \tag{3}$$

where C_o is the initial metal concentration. The value of R_L indicates the shape of isotherm to be either unfavorable ($R_L > 1$) or linear ($R_L = 1$) or favorable ($0 < R_L < 1$) or irreversible ($R_L = 0$).

The Freundlich equation is the empirical relationship whereby it is assumed that the adsorption energy of a metal binding to a site on an adsorbent depends on whether or not the adjacent sites are already occupied. This empirical equation takes the form:

$$q_e = K_F (C_e)^{1/n} \tag{4}$$

where K_F and n are the Freundlich constants, the characteristics of the system. K_F and n are the indicators of the adsorption capacity and adsorption intensity, respectively.

The experimental Hg(II) ion adsorption isotherm presented in Fig. 5 was fitted by the Langmuir and Freundlich isotherms. The equilibrium adsorption constants calculated from the corresponding isotherms with the correlation coefficients are presented in Table 1. Based on the adsorption experimental results, Langmuir and Freundlich model parameters (q_m, b and K_F, n) were determined with linear regression. The maximum adsorption capacity of Hg(II) calculated by Langmuir equation was 130.5 mg g^{-1} beads. The correlation coefficient of the Langmuir isotherm is higher than that of the Freundlich isotherm. The Langmuir constant (q_m) values fitted the experimental values. On the other hand, the magnitudes of K_F and n (Freundlich constants) showed easy separation of metal ions from aqueous medium and indicated favorable adsorption. As seen from Table 1, n values were found high enough for separation of heavy metal ions from aqueous medium. The conformity of the adsorption data to the Langmuir isotherm (correlation coefficient >0.99) could be interpreted as indicating a homogeny adsorption process, leading to monolayer binding (Fig. 6). Based on the effect of separation factor R_L values are in the range between 0.029 and 0.469, which indicates that the magnetic beaded material are favorable adsorbents for Hg(II) removal from aqueous solution.

The thermodynamic parameters of adsorption system were also evaluated. The dependency of the equilibrium association constant, $K_a = b$ (M^{-1}), versus $1/T$ for the binding of magnetic beads was analyzed in terms of van't Hoff plots. The enthalpy and entropy changes for adsorption system were determined from the slope and intercept, respectively ($\ln K_a = (\Delta S^\circ / R) - (\Delta H^\circ / RT)$). The values of ΔG° and ΔS° can be estimated from the relationships $\Delta G^\circ = -RT \ln K_a$ and $\Delta G^\circ = \Delta H^\circ - T\Delta S^\circ$. Change in the enthalpy, ΔH, for Hg(II) adsorption was 8.57 kcal mol^{-1}. The value of ΔH was positive,
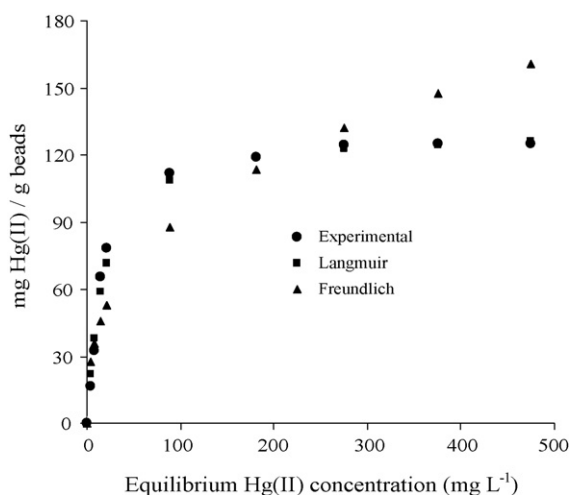

Fig. 5. Comparison of the equilibrium experimental and the adsorption isotherms obtained from the Langmuir and the Freundlich models for Hg(II) ion adsorption on the magnetic beads; volume of the medium: 50 mL; temperature: 298 K; pH: 5.5.

Table 1
The isotherm model constants and correlation coefficients of Hg(II) adsorption on the magnetic p(GMA-MMA-EGDMA) beads

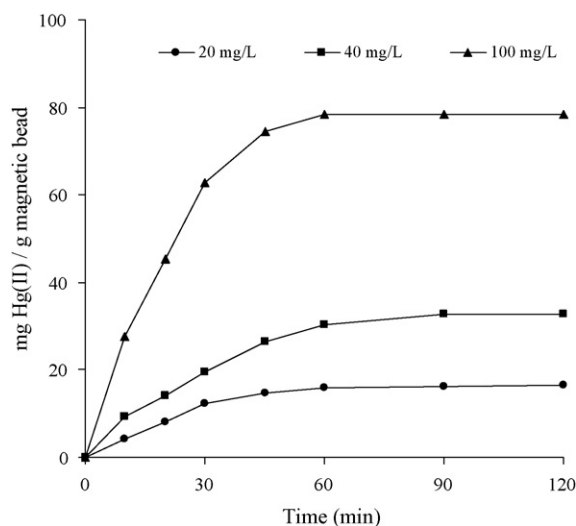| Temperature (K)	Experimental	Langmuir constant			Freundlich constant			ΔG
	q_{exp} (mg g^{-1})	q_m (mg/g)	$b \times 10^2$ (L mg^{-1})	R^2	K_F	n	R^2	(kcal mol^{-1})
288	102.5 ± 2.3	110.7	3.01	0.998	9.9	2.39	0.948	−5.00
298	124.8 ± 2.1	130.5	5.65	0.999	17.8	2.46	0.911	−5.56
308	132.5 ± 3.4	136.3	8.60	0.996	23.5	3.13	0.976	−5.97
323	143.7 ± 1.9	141.9	9.97	0.997	37.7	4.05	0.969	−6.67

Fig. 6. Effect of contact time for biosorption of Hg(II) ions on the magnetic beads. Volume of the medium: 50 mL; temperature: 298 K; pH: 5.5; adsorption time: 2 h.

implied that the process was endothermic. The entropy (ΔS) value for the adsorption was 47.08 cal mol^{-1}. Positive value of the ΔS was obtained in adsorption system, indicating an increase in the degree of adsorbate operative because of more randomness during adsorption process. The ΔG values were calculated for each temperature and in accordance with adsorption being a favorable process, the derived ΔG values, tabulated in Table 1 were all negative. The negative ΔG values for the adsorbent system implied that the adsorption process was spontaneous in nature [24,25].

3.4. Kinetics of adsorption

The adsorption of Hg(II) ions by the magnetic beads appears to be temperature dependent over the temperature range tested (288–323 °C) in our study. The adsorption capacity of Hg(II)

increases with increasing the temperature from 288 to 323 K (Table 2). The activation energy derived from Arrhenius equation, $k = A_o \exp(-E_a/RT)$ where A_o the temperature independent factor, k the second order rate constant and R is the gas constant (cal mol^{-1} K^{-1}), for the removal of Hg(II) was determined using equilibrium adsorption data at different temperatures. Value of the activation energy, E_a, can be calculated from the slope of $\ln k_2$ versus $1/T$ plot and is found to be 2.24 cal mol^{-1}.

In adsorption processes, there are several parameters which determine the adsorption rate, such as stirring rate in the aqueous phase or flow-rate in a column system, structural properties of adsorbent used (e.g., surface topography, porosity, swelling ratio), amount of the adsorbent, metal ion properties (e.g., hydrated ionic radius, coordination complex number), initial concentration of metal ions, and the existence of other metal ions which may compete with the metal ion of interest for the same active adsorption sites. As can be seen from Fig. 6, the Hg(II) ions removal rate was high at the beginning of adsorption and saturation levels were completely reached at about 60 min for Hg(II) ions. After this equilibrium period, the amount of adsorbed metal ions on the adsorbent did not significantly change with time. This trend in binding of metal ions suggests that the binding may be through interactions with functional groups located on the surface of the adsorbents.

Two reaction rate equations were used to analyze the adsorption kinetic of Hg(II) onto magnetic beads. The first-order rate equation of Lagergren is one of the most widely used for the adsorption of solute from a solution [26,27]. The model has the following form:

$$\log\left(\frac{q_{eq}}{q_{eq} - q_t}\right) = \frac{k_1 t}{2.303} \qquad (5)$$

where k_1 is the rate constant of first-order adsorption (min^{-1}) and q_{eq} and q_t denote the amounts of adsorption at equilibrium and at time t (mg g^{-1}), respectively. In a true first order process $\log q_{eq}$ should be equal to the intercept of a plot of $\log(q_{eq} - q_t)$ against t.

Table 2
The first-order and second-order kinetics constants for adsorption of Hg(II) on the magnetic beads

Temperature (K)	Experimental	First-order kinetic			Second-order kinetic		
	q_{exp} (mg g^{-1})	$k_1 \times 10^1$ (min^{-1})	q_{eq} (mg g^{-1})	R^2	k_2 (g mg min^{-1})	q_{eq} (mg g^{-1})	R^2
288	102.5 ± 2.3	0.58	76.3	0.976	0.14	107.5	0.988
298	124.8 ± 2.1	0.12	219.6	0.929	0.18	128.2	0.991
308	132.5 ± 3.4	0.11	286.1	0.898	0.20	135.1	0.989
323	143.7 ± 1.9	0.10	204.2	0.961	0.22	148.6	0.997

Ritchie proposed a method for the kinetic adsorption of gases on solids [28,29]. If metal ion adsorption medium is considered to be a second-order reaction, Ritchie equation is:

$$\left(\frac{1}{q_t}\right) = \left(\frac{1}{k_2 q_{eq} t}\right) + \left(\frac{1}{q_{eq}}\right) \tag{6}$$

where k_2 (g mg^{-1} min) is the rate constant of the second order adsorption.

The kinetic model parameters rate constant (k_2) and adsorption at equilibrium (q_{eq}) are presented in Table 2. The second-order kinetics best described the data. The theoretical q_{eq} values estimated from the first-order kinetic model gave significantly different value compared to experimental values. These results suggest that the second order mechanism is predominant and that chemisorption might be the rate-limiting step that controls the adsorption process. The rate-controlling mechanism may vary during the course of the adsorption process three possible mechanisms may be occurring. There is an external surface mass transfer or film diffusion process that controls the early stages of the adsorption process. This may be followed by a reaction or constant rate stage and finally by a diffusion stage where the adsorption process slows down considerably [30–33].

3.5. Operation of MFB reactor for removal of Hg(II) ions

For the continuous system application of the magnetic beads, the most convenient configuration can be that of a magnetically stabilized fluidized bed reactor (MFB). A large volume of water can be continuously treated using a defined quantity of adsorbent in the continuous reactor system. The continuous system operation parameter is presented in Section 2.5, and the residence time corresponding to the given flow rates is calculated by the following equation:

$$D = \frac{v_o}{\varepsilon V} \tag{7}$$

where D is the dilution rate (h^{-1}), v_o the volumetric flow-rate of the metal ion solution (ml h^{-1}), V the total volume of the continuous system (ml) and ε is the void fraction of given as ratio of void volume to the total volume of the continuous system. Residence time (τ) is the reciprocal of dilution rate.

The effect of flow-rate on the adsorption of Hg(II) ions by the aminated magnetic beads was investigated by fixing initial Hg(II) concentration 200 mg L^{-1} and keeping of flow-rate between 20 and 120 ml h^{-1}. Fig. 7 shows the effect of residence time on the adsorption efficiency of the Hg(II) ions by the aminated magnetic beads. As seen in figure, the adsorption efficiency of the magnetic beads decreased significantly from 139.4 ± 1.4 to 42.5 ± 1.1 mg g^{-1} beads with the decrease the residence time from 0.2970 to 0.0495 h. The results show that the adsorption of Hg(II) ions on to the beads was dependent on the residence time. As seen in the figure, the residence time is increased; the removal efficiency is also increased. At the highest flow-rate (i.e., lowest residence time), the lowest Hg(II) ions removal efficiency was observed. This behavior can be due to the insufficient contact time between Hg(II) ions and the aminated magnetic beads.
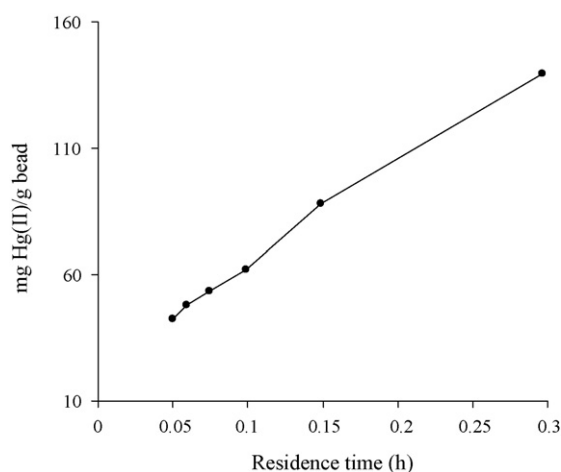

Fig. 7. Effect of residence time on Hg(II) ions adsorption in MFB reactor. Temperature: 298 K; pH: 5.5; initial concentration of metal ions: 200 mg L^{-1}.

In the continuous system with an 200 mg L^{-1} initial Hg(II) ions concentration, the adsorption capacity of the aminated magnetic beads was determined as 149.4 ± 3.8 mg g^{-1}. On the other hand, at the same initial concentration, the adsorption capacity for the same preparation was obtained as 124.8 ± 2.1 mg g^{-1} from the batch system. In the continuous system, the adsorption capacity of the adsorbent was about 20% higher than that of the batch system. The observed lower adsorption capacity in the batch systems may be resulted of the low equilibrium concentration of the Hg(II) ions compared to continuous system. In the continuous system, the concentration of the Hg(II) ions in the effluent increased gradually until the adsorptive sides of the adsorbent saturated with the Hg(II) ions. At saturation, the concentration of Hg(II) ions in the effluent was same as the inlet Hg(II) ions concentration. The driving force for adsorption is the concentration difference between the Hg(II) ions on the adsorbent and the Hg(II) ions in the solution [6,32–35]. Thus, the high driving force due to high Hg(II) ions concentration resulted in a better performance in the continuous system. For batch mode, the concentration of solute in contact with a specific quantity of adsorbent steadily decreases as adsorption proceeds, thereby decreasing the effectiveness of the adsorbent for removing the solute.

3.6. Regeneration and reuse

The aminated magnetic beads adsorbed Hg(II) ions were transferred in the desorption solution (10 mM HNO$_3$; 50 ml) and was stirred magnetically for 2 h. The final metal ion concentration in the aqueous phase was determined AAS. The elution ratio was calculated from the amount of metal ions adsorbed onto the beads and the final metal ions concentration in the desorption medium. Desorption ratios were very high (up to 93.6 ± 1.7%) when 10 mM HNO$_3$ solution is used as a desorption agent, the coordination adsorbent of chelated Hg(II) ions are disrupted and subsequently Hg(II) ions are released from the solid surface into the desorption medium. Therefore, we conclude that HNO$_3$ is a suitable desorption agent for the magnetic adsorbent, and,

aminated p(GMA-MMA-EGDMA) magnetic beads can be used repeatedly without significantly losing their adsorption capacities for the metal ions studied.

In order to show the reusability of the aminated magnetic beads; adsorption–desorption cycle of Hg(II) ions was repeated 10 times by using the same magnetic beads. The adsorption capacity of the magnetic beads did not noticeably change during the repeated adsorption–desorption operations. These results showed that magnetic beads could be repeatedly used in Hg(II) removal studies without detectable losses in their initial adsorption capacities.

4. Conclusions

Magnetic functional polymeric beads have been arisen great interest in the fields of biotechnology and biomedicine because they can be easily collected with application of a magnetic field, and the immobilization of appropriate ligands to such beads provide and effective tool to achieve rapid, simple and specific protein and cell separation [3,13,33]. Compared to conventional separation, the advantages of magnetic separation are attributed to its speed, accuracy, and simplicity. In this article, magnetic beads were prepared and used for the removal of Hg(II) ion in both batch and continuous systems. The magnetic beads showed a maximum adsorption at liquid phase pH 5.5. The magnetic beads a high magnetic responsiveness in magnetic field, and no aggregation of the particles was observed after magnetic field treatment. The mechanism and the kinetic of Hg(II) ions adsorption on the magnetic beads depend on the experimental conditions particularly medium pH and metal ions concentration. The equilibrium adsorption was well described by Langmuir adsorption isotherm. Equilibrium adsorption kinetics of Hg(II) on the magnetic beads obeyed the second-order kinetic. Hg(II) ions could be repeatedly adsorbed and desorbed without significant losses in their adsorption capacities. We can conclude that magnetic separation technique has a high application potential in the recovery of toxic heavy metal ions from aqueous solution and/or waste water system because of its high speed, low cost and suitability to the automation.

References

[1] C. Liu, R. Bai, Preparing highly porous chitosan/cellulose acetate membrane blend hollow fibers as adsorptive membranes: effect of polymer concentrations and coagulant compositions, J. Membr. Sci. 279 (2006) 336–346.

[2] F.M.M. Morel, A.M.L. Kraepiel, M. Amyot, The chemical cycle and bioaccumulation of mercury, Annu. Rev. Ecol. Syst. 29 (1998) 543–566.

[3] O. Genc, C. Arpa, G. Bayramoglu, M.Y. Arıca, S. Bektas, Selective recovery of mercury by Procion Brown MX 5BR immobilized poly(hydroxyethylmethacrylate/chitosan) composite membranes, Hydrometallurgy 67 (2002) 53–62.

[4] C. Jeon, W.H. Höll, Chemical modification of chitosan and equilibrium study for mercury ion removal, Water Res. 37 (2003) 4770–4780.

[5] M.E. Paez-Hernandez, K. Aguilar-Arteaga, C.A. Galan-Vidal, M. Palomar-Pardave, M. Remero-Romo, M.T. Ramirez-Silva, Mercury ions removal from aqueous solution using an activated composite membrane, Environ. Sci. Technol. 39 (2005) 7667–7670.

[6] G. Bayramoğlu, M.Y. Arıca, Ethylene diamine grafted poly(glycidyl methacrylate-co-methylmethacrylate) sorbent for removal of Cr(VI) ions, Sep. Pur. Technol. 45 (2005) 192–199.

[7] Z.M. Saiyed, S.D. Telang, C.N. Ramchand, Application of magnetic techniques in the field of drug discovery and biomedicine, Biomagn. Res. Technol 1 (2003) 1–8.

[8] Y. Ding, Y. Sun, Small-sized dense magnetic pellicular support for magnetically stabilized fluidized bed adsorption of protein, Chem. Eng. Sci. 60 (2005) 917–924.

[9] Z. Ma, Y. Guan, H. Liu, Superparamagnetic silica nanoparticles with immobilized metal affinity ligands for protein adsorption, J. Magn. Magn. Mater. 301 (2006) 469–477.

[10] M.Y. Arıca, G. Bayramoglu, M. Yılmaz, Ö. Genç, S. Bektaş, Biosorption of Hg²⁺, Cd²⁺ and Zn²⁺ by Ca-alginate and immobilized wood-rotting funguns Funalia trogii, J. Hazar. Mater. 109 (2004) 191–199.

[11] C. Haidouti, Inactivation of mercury in contaminated soils using natural zeolites, Sci. Total Environ. 208 (1997) 105–109.

[12] W. Mertz, The essential trace elements, Science 213 (1981) 1332–1338.

[13] M.Y. Arıca, H. Yavuz, S. Patır, A. Denizli, Immobilization of glucoamylase onto spacer-arm attached magnetic poly(methylmethacrylate) microspheres: characterization and application to a continuous flow reactor, J. Mol. Catal. B 11 (2000) 127–138.

[14] P.V. Finotelli, M.A. Morales, M.H. Rocha-Leao, E.M. Baggio-Saitovitch, A.M. Rossi, Magnetic studies of iron(III) nanoparticles in alginate polymer for drug delivery applications, Mater. Sci. Eng. C 24 (2004) 625–629.

[15] A.R. Cestari, C. Airoldi, Chemisorption on thiol-silicas: divalent cations as a function of pH and primary amines on thiol-mercury adsorbed, J. Coll. Interf. Sci. 195 (1997) 338–342.

[16] O. Genç, L. Soysal, G. Bayramoğlu, M.Y. Arıca, S. Bektaş, Procion Green H-4G immobilized poly(2-hydroxyethylmethacrylate/chitosan) composite membranes for heavy metal removal, J. Hazard. Mater. 97 (2003) 111–125.

[17] O. Genç, Y. Yalcınkaya, E. Büyüktuncel, A. Denizli, M.Y. Arıca, S. Bektaş, Uranium recovery by immobilized and dried powdered biomass: characterisation and comparison, Int. J. Min. Process. 68 (2003) 93–107.

[18] A. Denizli, S. Bektaş, M.Y. Arıca, O. Genç, Metal chelating properties of poly(hydroxyethylmethacrylate-co-methacryloamidohistidine) membrane, J. Appl. Polym. Sci. 97 (2005) 1213–1219.

[19] M.Y. Arıca, O. Genc, Entrapment of white-rot fungus Trametes versicolor in Ca-alginate beads: preparation and biosorption kinetics analysis for cadmium removal from aqueous solutions, Biores. Technol. 80 (2001) 121–129.

[20] M.Y. Arica, I. Tüzün, E. Yalın, O. Ince, G. Bayramoglu, Utilisation of native, heat and acid-treated microalge Chlamydomonas reinhardtii preparations for biosorption of Cr(VI) ions, Process Biochem. 40 (2005) 2351–2358.

[21] V.J.P. Vilar, C.M.S. Botelho, R.A.R. Boaventura, Influence of pH, ionic strength and temperature on lead biosorption by Gelidium and agar extraction algal waste, Process Biochem. 40 (2005) 3267–3275.

[22] G. Bayramoğlu, G. Celik, M.Y. Arıca, Studies on accumulation of uranium by fungus Lentinus sajor-caju, J. Hazard. Mater. 136 (2006) 343–351.

[23] W.S.W. Ngah, S. Ab Ghani, A. Kamari, Adsorption behavior of Fe(II) and Fe(III) ions in aqueous solution on chitosan and cross-linked chitosan beads, Biores. Technol. 96 (2005) 443–450.

[24] G. Bayramoğlu, A. Senel, M.Y. Arica, Effect of spacer arm and Cu(II) ions on performance of L-histidine immobilized on the poly(GMA/MMA) beads as a affinity ligand for separation and purification of IgG, Sep. Pur. Technol. 50 (2006) 229–239.

[25] G. Bayramoğlu, S. Bektas, M.Y. Arica, Biosorption of heavy metal ions on immobilized white-rot fungus Trametes versicolor, J. Hazard. Mater. 101 (2003) 285–300.

[26] S. Lagergren, About the theory of so-called adsorption of soluble substance, Kung Sven. Veten. Hand 24 (1898) 1–39.

[27] G. Bayramoğlu, I. Tuzun, G. Celik, M. Yilmaz, M.Y. Arica, Biosorption of mercury(II), cadmium(II) and lead(II) ions from aqueous system by microalgae Chlamydomonas reinhardtii immobilized in alginate beads, Int. J. Miner. Process. 81 (2006) 35–43.

[28] K.V. Kumar, S.S. Sivanesan, Equilibrium data, isotherm parameters and process desing for partial and complete isotherm of methylene blue onto activated carbon, J. Hazard. Mater. B 134 (2006) 237–244.

[29] A.G. Ritchie, Alternative to the Elovich equation for kinetics of adsorption of gases on solids, J. Chem. Soc., Faraday Trans. 73 (1987) 1650–1653.

[30] T. Akar, S. Tunali, Biosorption characteristics of *Aspergillus flavus* biomass for removal of Pb(II) and Cu(II) ions from an aqueous solutions, Biores. Tecnol. 97 (2006) 1780–1787.

[31] M.Y. Arica, G. Bayramoglu, N. Bicak, Characterization of tyrosinase immobilised onto spacer-arm attached glycidylmethacrylate-based reactive microbeads, Process Biochem. 39 (2004) 2007–2017.

[32] Z. Aksu, F. Gonen, Binary biosorption of phenol and chromium(VI) onto immobilized activated sludge in a packed bed: prediction of kinetic parameters and breakthrough curves, Sep. Pur. Technol. 49 (2006) 205–216.

[33] C.-Y. Chen, C.-L. Chiang, P.-C. Huang, Adsorption of heavy metal ions by a magnetic chelating resin containing hydroxyl and iminodiacetate groups, Sep. Pur. Technol. 50 (2006) 15–21.

[34] C.M. Sun, R.J. Qu, C.N. Ji, Q. Wang, C.H. Wang, Y.Z. Sun, G.X. Cheng, A chelating resin containing S, N and O atoms: synthesis and adsorption properties for Hg(II), Eur. Polym. J. 42 (2006) 188–194.

[35] A.A. Atia, A.M. Donia, K.Z. Elwakeel, Selective separation of mercury(II) using a synthetic resin containing amino and mercaptan as chelating groups, React. Funct. Polym. 65 (2005) 267–275.